https://doi.org/10.5194/egusphere-2025-1478
Preprint. Discussion started: 8 April 2025
© Author(s) 2025. CC BY 4.0 License.

Multidecadal trends in CO_2 evasion and aquatic metabolism in a large temperate river

An Truong Nguyen[1*], Gwenaël Abril[2,3], Jacob S. Diamond[1,4], Raphaël Lamouroux[5], Cécile Martinet[6], Florentina Moatar[1]

[1] INRAE, UR RiverLy, 5 Rue de la Doua, 69100 Villeurbanne, France

[2] Laboratoire de Biologie des Organismes et Ecosystèmes Aquatiques (BOREA), UMR 8067, Muséum National d'Histoire Naturelle, CNRS, IRD, SU, UCN, UA, Paris, France.

[3] Programa de Geoquímica, Universidade Federal Fluminense, Niterói, Rio de Janeiro, Brazil

[4] Dipartimento di Scienze Ambientali, Informatica e Statistica, University of Venice Ca' Foscari, Via Torino 155, 30172 Venezia Mestre, Italy

[5] EDF – Recherche et Développement, Laboratoire National d'Hydraulique et Environnement, Chatou, France

[6] EDF – Division Technique Générale, Electricité de France, Grenoble, France

[*] Corresponding author: An Truong Nguyen (truongan9393@yahoo.com, truong-an.nguyen@inrae.fr)

Abstract. Rivers play a critical role in the global carbon cycle. However, the environmental and hydro-climatic factors that control the sign and magnitude of river CO_2 fluxes across seasons and multi-decadal periods are less constrained. The origin of excess river CO_2—delivered by soils, wetlands and groundwater or produced by aquatic respiration of organic matter—remains an important unknown in linking terrestrial and aquatic carbon budgets. To address these knowledge gaps, we report on a 32-year high-frequency dataset (1990–2021) from the Loire River, a large, temperate river that underwent a shift from a eutrophic, phytoplankton-dominated regime to an oligotrophic, macrophyte-dominated regime in ca. 2005. We estimated daily river-atmosphere CO_2 flux (FCO_2) and river net ecosystem productivity (NEP) from hourly pH, alkalinity, dissolved oxygen, water temperature and solar radiation. We demonstrate that: i) annual FCO_2 varied an order of magnitude among years (range = 200–2600 g C m^2 yr^{-1}); ii) the mean annual contribution of aquatic metabolism to total FCO_2 was 40%, but this also varied according to year and trophic regime, ranging from negative to 100% contribution; iii) the river occasionally acted as a CO_2 sink ($FCO_2 < 0$) during summer, especially during the eutrophic period of 1990-2000, but this flux was negligible (-0.6% of the FCO_2 budget); and iv) FCO_2 exhibited hysteresis with discharge, with FCO_2 levels ranging from 1.5 to 2 times higher in autumn compared to spring at equivalent discharge rates, and the degree of which was depended on trophic regime. This study makes

© Author(s) 2025. CC BY 4.0 License.

clear that river FCO_2—and the source of this CO_2—is dynamic within and across years and that global changes affecting the river trophic regime control the balance between internal and external CO_2 production.

Keywords: internal contribution, autotrophic, heterotrophic, long-term trend, metabolic shift, Loire River

1. Introduction

Streams and rivers contribute 60% (1.8 Pg C yr^{-1}) of CO_2 evasion from all inland waters (Raymond et al., 2013). Most CO_2 flux (FCO_2) emitted comes from "external" sources, delivered to streams via groundwater inputs and via temporary hydrologic connectivity with riparian wetlands (Abril & Borges, 2019; Hotchkiss et al., 2015). Additional, geochemical weathering and photochemical processes are also considered external sources to river FCO_2 (Hotchkiss et al., 2015). While geochemical weathering primarily affects river alkalinity and indirectly influences CO_2 dynamics through changes in water chemistry (Jones et al., 2003), photochemical processes make a relatively minor contribution to CO_2 production when compared to biological processes (Amaral et al., 2013; Koehler et al., 2014). The remainder of FCO_2 from rivers originates from in-stream respiration of organic matter (Cole et al., 2001), termed the "internal" source of CO_2. While the balance between internal versus external CO_2 sources is spatially predictable (Hotchkiss et al., 2015), its temporal variation is less clear. Most analyses on the origin of stream FCO_2 occur over one season (e.g., Bernal et al., 2022; Rocher-Ros et al., 2020) or rely on discrete samplings (e.g., Hotchkiss et al., 2015). Recent work by Young et al. (2025) highlighted this complexity by documenting strong seasonal variability driven by hydrological events, temperature fluctuations, and biological productivity in a temperate river. Their four-year study emphasized the need for longer-term datasets to capture interannual variability, particularly in the context of ongoing climate and ecological changes. The seasonal hydrology plays an important role in determining the magnitude and timing of CO_2 emissions from rivers, as changes in flow rates affect the transport of nutrient, organic carbon from surrounding land as input for stream metabolism and the exchange of CO_2 between the river and the atmosphere (Cole et al., 2007; Hotchkiss et al., 2015). There is thus a lack of understanding of the temporal variability of FCO_2 and its sources, which are increasingly crucial under a changing climate that increases water temperature and modifies river flow (Floury et al.,

https://doi.org/10.5194/egusphere-2025-1478
Preprint. Discussion started: 8 April 2025
© Author(s) 2025. CC BY 4.0 License.

2012; Van Vliet et al., 2013). This knowledge gap is most prominent in large rivers, leading to significant uncertainty in global FCO_2 assessment from inland waters (Battin et al., 2023; Hotchkiss et al., 2015).

The relative contribution of internal CO_2 sources can be quantified as the ratio between net ecosystem productivity (NEP) and FCO_2. NEP is the balance between gross primary production (GPP) and ecosystem respiration (ER) (NEP = GPP – ER). When NEP is negative (GPP < ER), the river is in a "heterotrophic" state, and CO_2 is added to the water column by net organic matter respiration. Assuming the river is a CO_2 source (FCO_2 > 0) and in a heterotrophic state, the –NEP/FCO_2 ratio yields the ratio of internal source contribution to total emissions, and by difference, the ratio of external CO_2 source contribution (=1+ NEP/FCO_2). This ratio can be evaluated in response to environmental drivers such as hydrology (Hotchkiss et al., 2015), light (Rocher-Ros et al., 2021), water temperature (Lynch et al., 2010; Wallin et al., 2020), and organic matter source (Bernal et al., 2022; Reed et al., 2021). However, rivers are not always CO_2 sources and can seasonally function as CO_2 sinks when high rates of GPP deplete CO_2, leading to CO_2 undersaturation (Aho et al., 2021; Zhang et al., 2017). In this "autotrophic" state (GPP > ER), positive NEP yields local organic matter increases. This period is most common in larger rivers but is typically missed by FCO_2 sampling campaigns, furthering the need for high-frequency, long-term studies of coupled stream metabolism and CO_2 measurements.

Autotrophic periods were common in large rivers throughout the 1980s and 1990s, characterized by high nutrient concentrations and high chlorophyll-*a* (i.e., an eutrophic regime) (Dodds & Smith, 2016). The Loire River (France) was classified as the most eutrophic in Europe at that time (Minaudo et al., 2015; Moatar & Meybeck, 2005). Despite potential autotrophic activity, the CO_2 dynamics during these periods remains poorly documented due to the lack of comprehensive CO_2 data, leaving a gap in our understanding of whether the river predominantly acted as a CO_2 source or sink.

From 1990 to 2005, the Loire River underwent ecological shifts from planktonic autotrophic communities dominated by phytoplankton to benthic communities dominated by rooted macrophytes (Minaudo et al., 2015), which is termed "re-oligotrophication" (Ibáñez et al., 2022). The ecosystem transition was accompanied by a delayed shift in the river metabolic regime in 2012–2014, associated with reductions in GPP and NEP in the growing season (Diamond et al., 2022). As a result,

https://doi.org/10.5194/egusphere-2025-1478
Preprint. Discussion started: 8 April 2025
© Author(s) 2025. CC BY 4.0 License.

approximately 10% of NEP was decreased (Diamond et al., 2022), which could potentially lead to an increase in FCO_2 due to decreased CO_2 consumption by stream metabolism. As re-oligotrophication may become increasingly common in developed countries, its effects on FCO_2 and CO_2 source variation remain unknown.

In this study, we used a 32-year daily dataset of coupled stream metabolism (NEP) and FCO_2 to assess the temporal internal/external CO_2 source contributions in the Loire River. We hypothesized that the FCO_2 and its internal source contribution would increase following the re-oligotrophication ecosystem shift. Specifically, we predicted that these increases would manifest coincidentally with the shifts in phytoplankton to macrophyte-dominated in 2005 and stream metabolism regime in 2012. Finally, because GPP under macrophytes is less flow-dependent than under phytoplankton (Diamond et al., 2022), we predicted that discharge would become a weaker control on FCO_2 in the macrophyte-dominated state, but this changing control would vary seasonally.

2. Methods

2.1. Study site

The study site (47.6°N, 2.6°E) is located in the middle Loire River, France, 564 km from the source, with a mean discharge of 300 m^3 s^{-1} (Supplementary Figure S1). Its 36,000 km² catchment is home to over two million residents. The land cover consists of forests (42%), pasture (35%), and agriculture (21%) (Moatar & Meybeck, 2005). The Loire River and its tributaries, upstream Dampierre drains volcanic, granitic area and sedimentary basins characterized by extensive limestone and marl formations (Figure S1). After the confluence with Allier River (100 km upstream of the study site), the carbonate-rich catchment and its interaction with the Loire River significantly contribute to river alkalinity primarily through the dissolution of carbonate minerals (Binet et al., 2022). Soil types within the Loire catchment are heterogeneous and their nature is closely linked to the underlying lithology. In addition, the catchment includes significant areas of alluvial deposits, which feature more fertile and productive soils for extensive agriculture in the region (Moatar et al., 2022; Moatar & Meybeck, 2005). This river is an 8th-order river with an anabranching fluvial pattern resulting from a gentle slope (0.4 m km^{-1}). During summer, the study site is shallow (1 m) and wide (330 m). The anabranching fluvial pattern leads

https://doi.org/10.5194/egusphere-2025-1478
Preprint. Discussion started: 8 April 2025
© Author(s) 2025. CC BY 4.0 License.

to a broad range of lateral hydrologic connectivity between the main channel and secondary channels colonized by semi-terrestrial vegetation (Janssen et al., 2023). These vegetated side channels may behave like floodplains by acting as seasonal sources of organic carbon (Abril & Borges, 2019).

2.2. Data acquisition and processing

Hourly data of pH, temperature, electrical conductivity (EC) at 25°C, and dissolved oxygen (DO) from 1990–2021 were extracted from the monitoring program conducted by Électricité de France (EDF) upstream and downstream of the nuclear power plant Dampierre (47.6°N, 2.6°E). Total alkalinity (TA) in the upstream station was measured at varying intervals, ranging from every three days to weekly, by EDF and Naiades (www.naiades.eaufrance.fr). We reconstructed the daily TA based on the linear relationship between EC and TA (Supplementary Figure S2). This study used the upstream data to calculate daily FCO_2 and NEP, while the downstream data was used to support the data cleaning procedure (Supplementary section S1).

We obtained daily global radiation data (W m^{-2}) from a nearby meteorological station (donneespubliques.meteofrance.fr). Mean daily discharge (m^3 s^{-1}) and river depth (m) were obtained from www.hydro.eaufrance.fr.

2.3. NEP and FCO_2 estimation

2.3.1. Metabolism estimation

We estimated daily GPP, ER (mmol C m^{-2} d^{-1}), and the gas exchange rate coefficient (K_{600}, d^{-1}) by using the inverse modelling approach that yields the best fit between modeled and observed DO. To avoid the unrealistic estimates, the K_{600} is constrained by daily river discharge and river depth with the formulations proposed by Raymond et al, 2012, while the hourly DO, solar radiation and daily water temperature data are required to further reduce equifinality of GPP, ER and K_{600}. These estimates are supported by the *streamMetabolizer*, a R package (Appling et al., 2018). The model setup for the Loire River was described by Diamond et al. (2021). About 12% of samples (n=1391) were discarded due to physically impossible results in metabolism estimation (i.e., negative values). Missing mean daily GPP and ER were then replaced by their daily 75th estimated percentile values provided by

https://doi.org/10.5194/egusphere-2025-1478
Preprint. Discussion started: 8 April 2025
© Author(s) 2025. CC BY 4.0 License.

streamMetabolizer, as detailed in Supplementary section S3. We imputed the remaining 1.7% of missing data using the rolling 7-day average. The covariance between estimated ER and K600 was low (R^2 = 0.09), demonstrating reduced influence of equifinality problem (Appling et al., 2018).

2.3.2. pCO_2 and FCO_2 estimation

Daily concentrations of partial pressure of CO_2 (pCO_2, µatm) were estimated by pyCO2SYS, a Python package for the CO2SYS model (Humphreys et al., 2022), using mean daily pH, water temperature, and TA. Carbonate dissociation constants K_1 and K_2 were chosen based on freshwater estimates (Millero, 1979). CO2SYS freshwater pCO_2 estimates are valid for water with TA > 1000 µmol L^{-1}, and results have been previously validated for the Loire River (2–9% bias) (Abril et al., 2015). The daily TA data in this study were estimated from daily EC with an average error of 190 µmol L-1, leading to an uncertainty in pCO2 estimation. PyCO2SYS can estimate pCO2 uncertainty by propagating the TA uncertainty (Humphreys et al., 2022). Uncertainty of estimated TA leads to ±11% uncertainty in pCO2 estimation, however there is no significant difference in the river CO2 state compared over 32 years (Supplementary section S4).

The FCO_2 (mmol C m^{-2} d^{-1}) between the water and the atmosphere was calculated using Fick's law, using the CO_2 transfer velocity (kCO_2, m d^{-1}) and the air-water CO_2 gradient (mmol m^{-3}) (Eq. 1). We obtained kCO_2 (Eq. 2) using Schmidt number (Sc) at given water temperature (Eq. 3) scaling from the gas transfer velocity k_{600} (m d^{-1}) (Raymond et al., 2012). The k_{600} was calculated by multiplying with river depth with K_{600}, an output of *streamMetabolizer*. We compared k_{600} with seven fitted equations proposed by Raymond et al., (2012) for streams and small rivers and found that they are within the same order of magnitude (Supplementary Figure S5). The k600 estimates from the StreamMetabolizer model were selected for FCO_2 calculations to ensure consistency with the NEP calculations.

$$FCO_2 = k_{\mathrm{CO_2}} \times (\mathrm{CO_2}_{\,\mathrm{water}} - \mathrm{CO_2}_{\,\mathrm{air}}) \qquad \text{Eq. 1}$$

$$k_{\mathrm{CO_2}} = depth\ \times K_{600}/\left(600/\mathrm{Sc}_{\mathrm{CO_2}}\right)^{-0.5} \qquad \text{Eq. 2}$$

https://doi.org/10.5194/egusphere-2025-1478
Preprint. Discussion started: 8 April 2025
© Author(s) 2025. CC BY 4.0 License.

$$\mathrm{Sc}_{CO_2} = 1911.1 - (118.1 \times T) + (3.45 \times T^2) - (0.0413 \times T^3) \qquad \text{Eq. 3}$$

$CO_{2,water}$ is aqueous CO_2 (mmol m^{-3}) estimated by pyCO2SYS, and $CO_{2,air}$ is CO_2 in equilibrium with the atmosphere using global monthly atmospheric CO_2 from 1990–2021 from National Oceanic and Atmospheric Administration Global Monitoring Laboratory (https://gml.noaa.gov/ccgg). We used Henry's law to convert pCO_2 in µatm into CO_2 in mmol m^{-3} using temperature-dependent solubility constants.

2.3.3. Categorizing NEP-FCO₂ states by autotrophic/heterotrophic and source/sink states

We categorized the river into four trophic-flux states (or "trophlux" states) based on daily NEP and FCO_2. If NEP is positive (GPP > ER), the river is autotrophic, while if NEP is negative (GPP < ER), the river is heterotrophic. Likewise, if FCO_2 is positive, the river is a CO_2 source, while if FCO_2 is negative, the river is a CO_2 sink, relative to the atmosphere. The river could thus be in four possible trophlux states: 1) autotrophic-sink, 2) autotrophic-source, 3) heterotrophic-sink, and 4) heterotrophic-source. The autotrophic-sink and heterotrophic-source states imply that NEP and FCO_2 vectors are moving CO_2 in the same direction, into water column biomass or out of the water column, respectively (Bogard & Del Giorgio, 2016). The remaining two states imply opposite directions between NEP and FCO_2. The autotrophic-source state implies that although there is a net conversion of CO_2 into biomass, there is a surplus of water column CO_2 relative to autotrophic needs, leading to continued positive FCO_2. The heterotrophic-sink state implies that despite the net conversion of biomass into water column CO_2, there is still a CO_2 undersaturation relative to the atmosphere, likely due to prior autotrophic uptake. We expect the heterotrophic-sink state to be a temporary occurrence, reflecting temporal lags within the carbonate system buffering capacity during the short transition between autotrophic and heterotrophic states. Conventionally, the aquatic metabolism contribution to river CO_2 emissions (i.e., the internal CO_2 source) is calculated as –NEP/FCO_2 in the heterotrophic-source state (Bernal et al., 2022; Hotchkiss et al., 2015; Kirk & Cohen, 2023).

https://doi.org/10.5194/egusphere-2025-1478
Preprint. Discussion started: 8 April 2025
© Author(s) 2025. CC BY 4.0 License.

2.4. Change points and long-term trend analysis

To test our hypothesis that FCO_2 would vary as a function of ecosystem state and metabolism shifts in the Loire River, we compared change points in FCO_2 with previously estimated change points in ecosystem state (ca. 2005) and metabolic regime (ca. 2012) (Diamond et al., 2022; Minaudo et al., 2015). We used the *ruptures* Python package (Truong et al., 2020) with a five-year window interval to ensure that identified changes were sustained beyond year-to-year variation. The change point detection was also applied to the daily NEP and related variables (pH, alkalinity, pCO_2, k600, GPP, and ER). We also conducted change point detection on seasonal decomposed time series of daily FCO_2 and NEP using the *statsmodels* Python package (Seabold & Perktold, 2010) to better identify changes in seasonal–as opposed to long-term–variations. We further estimated long-term trends of FCO_2 and NEP as functions of hydroclimatic conditions (discharge, water temperature) in each trophlux state by using the Mann-Kendall test (*pyMannKendall* Python package) (Hussain & Mahmud, 2019).

2.5. Seasonal hysteresis of NEP and FCO_2 in response to discharge changes

To test the influence of discharge on CO_2 emissions, we evaluated the hysteresis of mean daily FCO_2 and NEP against mean daily discharge across the periods delineated by the change point analysis. We predicted that for the same discharge, FCO_2 would exhibit a range of magnitudes depending on the season but that this range would decrease systematically as a function of decreasing phytoplankton coverage in the Loire River. We evaluated the hysteresis loops by the direction of hysteresis (clockwise or counterclockwise) and the magnitude (i.e., difference of FCO_2 at the same discharge but in the rising and falling flow stage). We additionally calculated hysteresis magnitude for –NEP, external source contribution (FCO_2 + NEP), and –NEP/FCO_2 at the mean discharge (300 m^3 s^{-1}, Table 2) during the rising (autumn) and falling stage (spring).

3. Results

3.1. Daily, seasonal, inter-annual FCO_2 emissions and NEP contribution for 32 years

FCO_2 and NEP exhibited strong daily, seasonal, and inter-annual variations (Figure 1). The pronounced seasonal variability resulted in the successive transition of different states of FCO_2 and NEP

https://doi.org/10.5194/egusphere-2025-1478
Preprint. Discussion started: 8 April 2025
© Author(s) 2025. CC BY 4.0 License.

(autotrophic/heterotrophic of NEP, sink/source of FCO_2) but with a recurring seasonal pattern each year (Figure 1c).

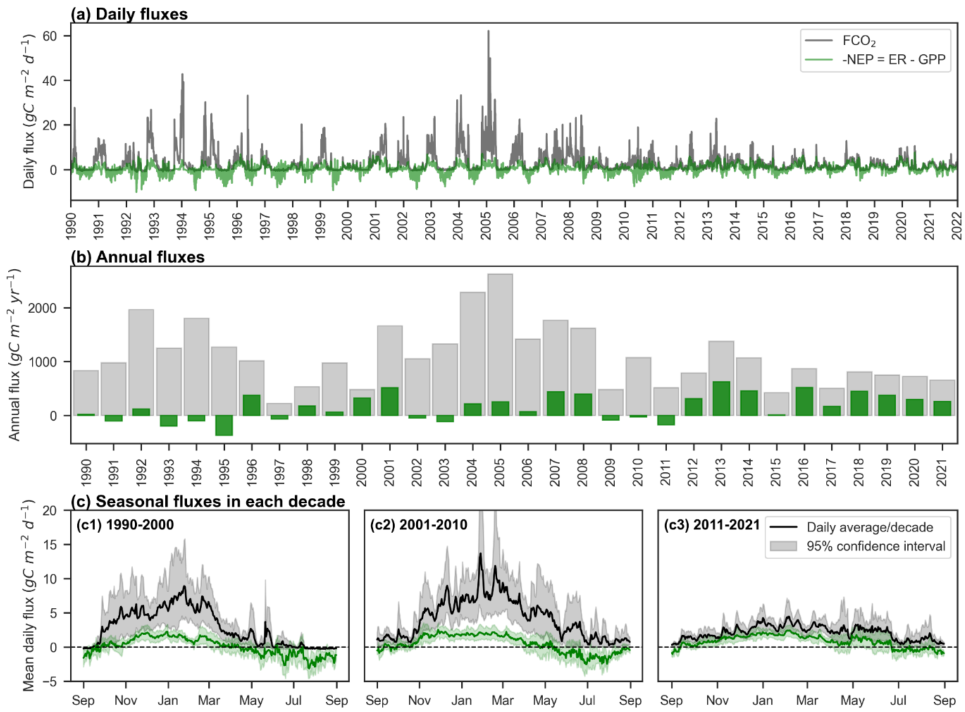

Figure 1. Evolution of FCO_2 and –NEP during 1990-2021. (a) Daily values (g C m^{-2} d^{-1}), (b) Cumulative annual fluxes (calendar year, g C m^{-2} y^{-1}), (c) Seasonal fluxes during hydrological year in each decade 1990-2000, 2001-2010, 2011-2021. In Figure 1c, the solid line and shaded area are the average and the 95% confidence interval of the daily fluxes each decade, calculated by 10 daily fluxes in the same day-year.

The daily average FCO_2 was 3 g C m^{-2} d^{-1}, with high peaks reaching 20 - 60 gC m^{-2} d^{-1} during high flow in winter (1000–2000 m^3 s^{-1}) and low peaks with negative FCO_2 of -0.8 gC m^{-2} d^{-1} during the low flow in summer (<150 m^3 s^{-1}) (Figure 1). The daily NEP was -0.45 gC m^{-2} d^{-1}, with average peaks from -4.0 gC m^{-2} d^{-1} in winter to 3.6 C m^{-2} d^{-1} in summer (Figure 1a).

Cumulative annual FCO_2 ranged from 221 to 2633 g C m^{-2} y^{-1} and NEP from -383–584 g C m^{-2} y^{-1}. Notably, there were 10 years from 1990–2011 when the Loire River was net autotrophic (Figure 1b, green bars). Even during these years, the Loire River was a source of CO_2 to the atmosphere (Figure 1b, grey bars). The contribution of external CO_2 sources (FCO_2 + NEP) ranged from 800–2400 g C m^{-2} y^{-1}

https://doi.org/10.5194/egusphere-2025-1478
Preprint. Discussion started: 8 April 2025
© Author(s) 2025. CC BY 4.0 License.

in 1990–2010. However, the contribution of external CO_2 sources has significantly decreased to ca. 400 g C m^{-2} y^{-1} since 2011 (Figure 1b).

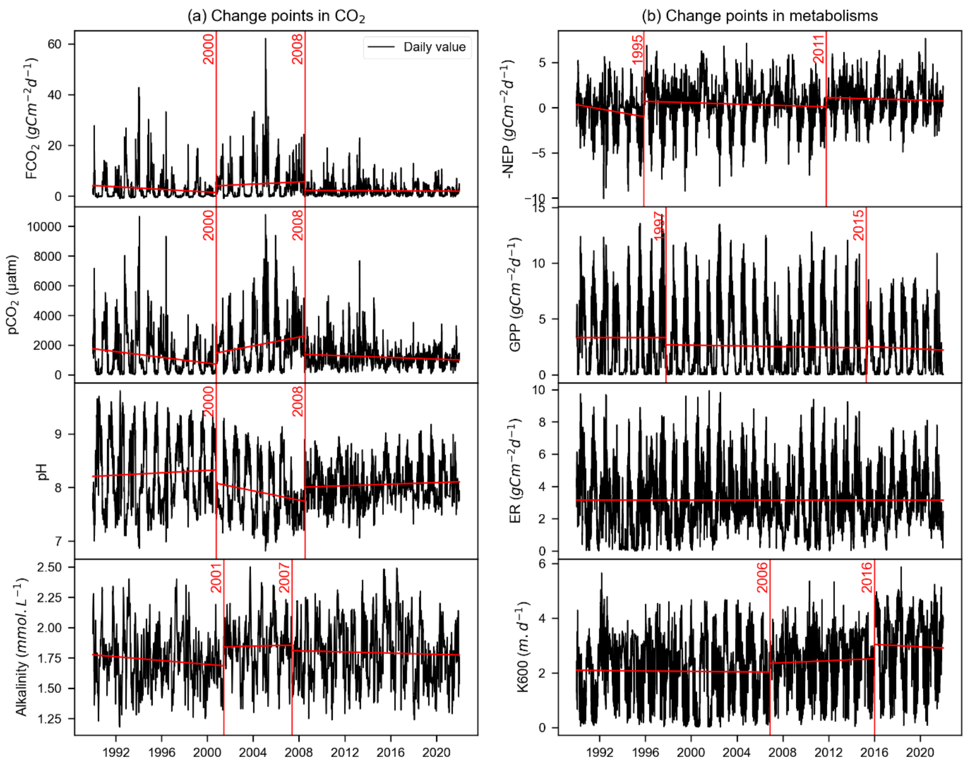

Figure 2. Change point detection in the daily time series of (a) FCO_2, pCO_2, pH, alkalinity and (b) –NEP, K600, GPP, ER during 1990-2021. The vertical red lines indicate the year of the change point.

The change point analysis on daily time series detected that the FCO_2 experienced two change points in 2000 and 2008 (Figure 2a), while the change points of –NEP were detected in 1995 and 2011 (Figure 2b). While change points in –NEP described a gradual increase, change points in FCO_2 indicated more abrupt fluctuations, with abnormal decrease in 2000 and 2008. The daily time series of pCO_2, pH, and alkalinity had similar change points to FCO_2. The change points of –NEP were mainly dependent on GPP, while no significant change in ER time series (Figure 2b). In addition, the seasonal decomposition analysis detected the same change point in 2008 for the seasonal amplitude in both FCO_2 and NEP, indicating a significant decrease in the seasonal variations (Supplementary Figure S6).

https://doi.org/10.5194/egusphere-2025-1478
Preprint. Discussion started: 8 April 2025
© Author(s) 2025. CC BY 4.0 License.

The periods of change in both FCO_2 and NEP spanned roughly three decades: (i) 1990–2000, (ii) 2001–2010, and (iii) 2011–2021. These time frames were selected based on changepoint analysis, which identified shifts in FCO_2 around 2000 and 2008, in NEP around 1995 and 2011, and GPP around 1997 and 2015 (Figure 2). Despite some discrepancies in the exact timing of these changepoints between FCO_2 and NEP, grouping the data by decades allowed for a coherent comparison of long-term trends in ecosystem behavior. These periods corresponded to distinct phases in river metabolism and CO_2 emissions: (i) high primary productivity (cumulative annual GPP= 1113 ± 225 g C m^{-2} y^{-1}, ER= 1136 ± 241 g C m^{-2} y^{-1}) and low CO_2 emission (FCO_2 = 1031 ± 531 g C m^{-2} y^{-1}) ; (ii) reduced primary productivity (GPP= 973 ± 292 g C m^{-2} y^{-1}, ER= 1136 ± 128 g C m^{-2} y^{-1}) and high CO_2 emission (FCO_2 = 1534 ± 620 g C m^{-2} y^{-1}), and (iii) low primary productivity (GPP= 867± 212 gC m^{-2} y^{-1}, ER= 1167 ± 163 g C m^{-2} y^{-1}) and low CO_2 emission (FCO_2 = 773 ± 272 g C m^{-2} y^{-1}).

3.2. Occurrence and contribution of trophlux states to CO_2 emissions

At the seasonal time scale, the Loire River varied among trophlux states, with the heterotrophic-source state predominating. The source state occurred the least (64% of time) in the first decade delineated by change points (1990–2000) and occurred the most (92% of time) in the most recent decade (2011–2021). Likewise, the heterotrophic state occurred at a minimum of 54% and a maximum of 67% of time during those decades, respectively. The joint occurrence of the heterotrophic-source state thus ranged from 47% to 66% of time (Table 1), coinciding with low water temperature and high discharge. This state contributed more than 90% of total annual CO_2 emissions. Within this state, internal sources contributed an average of 28–57% of total annual CO_2 emissions, implying external CO_2 source contributions of 72–43% in the Loire River.

The remaining three trophlux states contributed less than 10% to total FCO_2 despite their regular occurrence (e.g., up to 50%) during the 1990-2000 decade. There were often 1–3 months of CO_2 sink state due to high GPP in the summer growing season, coinciding with the highest water temperatures and the lowest discharge (Table 1). The autotrophic-sink reduced annual FCO_2 by 3% during 1990–2000 and by 0.3% in 2011–2021. In spring and autumn, the Loire River was regularly in an autotrophic state (17% to 28% of time) but remained a CO_2 source, presumably attributed to external CO_2 sources.

https://doi.org/10.5194/egusphere-2025-1478
Preprint. Discussion started: 8 April 2025
© Author(s) 2025. CC BY 4.0 License.

This autotrophic/source state contributed 8.2–9.2% to annual FCO_2 across years. The heterotrophic-sink state occurred rarely (1–7% of time) and had a small influence on the annual FCO_2 budget (0.1–0.8%). This state typically occurred as relatively short events of 1–14 days from June to August during the transition from autotrophic-sink state or heterotrophic-source state.

Table 1. Summary of the occurrence, fluxes, and related hydroclimatic conditions of each trophlux state in three decades 1990-2021. The values within the table are depicted as the mean annual value ± standard deviation, calculated for each decade (N=10 or 11).

Variable	Period	CO_2 source		CO_2 sink		All states
		Heterotrophic	Autotrophic	Heterotrophic	Autotrophic	
Occurrence (% of days)	1990-2000	47.3 ± 9.4	16.7 ± 9.2	7.3 ± 5.4	28.7 ± 7.0	100
	2001-2010	61.2 ± 12.7	25.3 ± 11.2	1.7 ± 1.1	15.5 ± 9.0	100
	2011-2021	65.8 ± 11.3	26.2 ± 8.6	1.1 ± 1.5	7.3 ± 5.7	100
FCO_2 budget (% of annual flux by each state)	1990-2000	94.6 ± 13.8	9.2 ± 11.4	-0.8 ± 1.4	-3.0 ± 4.2	100
	2001-2010	92.4 ± 11.3	8.2 ± 11.2	-0.1 ± 0.0	-0.6 ± 0.5	100
	2011-2021	91.8 ± 5.6	8.7 ± 5.8	-0.1 ± 0.2	-0.4 ± 0.3	100
–NEP ($gC\ m^{-2}\ y^{-1}$)	1990-2000	277 ± 158	-54 ± 46	25.5 ± 28.0	-225 ± 97	23 ± 222
	2001-2010	376 ± 127	-111 ± 83	3.8 ± 3.0	-131 ± 100	162 ± 234
	2011-2021	417 ± 173	-82 ± 48	2.0 ± 2.4	-36 ± 35	300 ± 232
FCO_2 ($gC\ m^{-2}\ y^{-1}$)	1990-2000	954 ± 514	102 ± 148	-4.4 ± 4.5	-21 ± 12	1031 ± 531
	2001-2010	1453 ± 666	88 ± 104	-0.6 ± 0.8	-7.8 ± 5.4	1534 ± 620
	2011-2021	717 ± 274	59 ± 28	-0.9 ± 1.8	-2.6 ± 2.1	773 ± 272
External CO_2 ($gC\ m^{-2}\ y^{-1}$)	1990-2000	677 ± 477	157 ± 92	-29 ± 32	204 ± 93	1008 ± 551
	2001-2010	1077 ± 595	199 ± 172	-4 ± 1	123 ± 95	1372 ± 528
	2011-2021	299 ± 140	140 ± 55	-2 ± 3	34 ± 31	472 ± 129
–NEP/FCO_2 (%)	1990-2000	37 ± 27	-123 ± 122*	-697 ± 546	1535 ± 1413**	5 ± 29
	2001-2010	28 ± 9	-195 ± 137*	-925 ± 786^{NS}	1983 ± 828**	7 ± 15
	2011-2021	57 ± 10	-150 ± 59*	-9204 ^{NS}	1480 ± 740**	34 ± 27
Temperature (°C)	1990-2000	8 ± 4	12 ± 4	18 ± 3	20 ± 3	13 ± 6
	2001-2010	10 ± 5	18 ± 5	18 ± 7	21 ± 3	13 ± 7
	2011-2021	11 ± 5	18 ± 5	10 ± 9	21 ± 3	14 ± 6
Discharge ($m^3\ s^{-1}$)	1990-2000	454 ± 326	276 ± 225	115 ± 60	111 ± 56	301 ± 290
	2001-2010	436 ± 323	160 ± 110	137 ± 69	115 ± 59	323 ± 296
	2011-2021	362 ± 278	120 ± 87	205 ± 136	80 ± 63	277 ± 259

* During the autotrophic/source state, the positive NEP reduces the outgassing of external CO_2, leading to a negative percentage ratio.

** The positive percentage ratio larger than 100% occurs during the autotrophic/sink state, where positive NEP involves the consumption of both external CO_2 and the CO_2 supplied from the atmosphere through the gas exchange at the air-water interface.

^{NS} Not significant –NEP/CO_2 ratio calculation is due to the rare heterotrophic-sink occurrence.

The external CO_2 ($gC\ m^{-2}\ y^{-1}$) = FCO_2 + NEP

https://doi.org/10.5194/egusphere-2025-1478
Preprint. Discussion started: 8 April 2025
© Author(s) 2025. CC BY 4.0 License.

3.3. The inter-annual trend of FCO_2 depending on trophlux states

The occurrence of heterotrophic-source and autotrophic-sink and their contribution to FCO_2 gradually changed from 1990–2021 (Figure 3). The occurrence of heterotrophic-source state increased from 140 days in 1990 to 250 days in 2021 (Figure 3a). However, the annual flux of –NEP within this state remained relatively stable (Figure 3b), while FCO_2 decreased with an average rate of 0.16 g C m^2 d^{-1} per year, resulting in a 62% reduction of FCO_2 in the heterotrophic-source state over the 32 years (Figure 3d). The annual decline in FCO_2 was uncorrelated (R^2 = 0.09) with the increase in annual water temperature (+5.7 °C/32 years), but it was positively correlated (R^2 = 0.36) with the decrease in annual discharge (-13%/32 years) (Table S2). Since the annual –NEP remained stable and FCO_2 decreased, the ratio of –NEP/FCO_2 thus increased from 20–40% in the 1990s to 60-75% in recent years, +1.25% per year (Figure 3f). There were some abnormal increases of –NEP/FCO_2 observed in 1995–2000, with the ratio reaching 100% in 1997 and 90% in 1996, 2000. These peaks were associated with a significant drop in FCO_2 (Figure 3d) and, thus, in external CO_2 sources (Figure 3b).

The autotrophic-sink state occurrence decreased from 140 days in 1990–2000 to 30 days in recent years (Figure 3a), following a reduction in +NEP from about 2 to 1.5 gC m^{-2} d^{-1} (-25%/32 years), corresponding to -0.015 g C m^2 d^{-1} per year (Figure 3b). In this state, annual discharge and temperature did not show significant changes ($p > 0.05$) (Figure 3c, e). The decrease in +NEP was not correlated with annual discharge (R^2 = 0.03) and annual temperature (R^2 = 0.00) (Table S2).

https://doi.org/10.5194/egusphere-2025-1478
Preprint. Discussion started: 8 April 2025
© Author(s) 2025. CC BY 4.0 License.

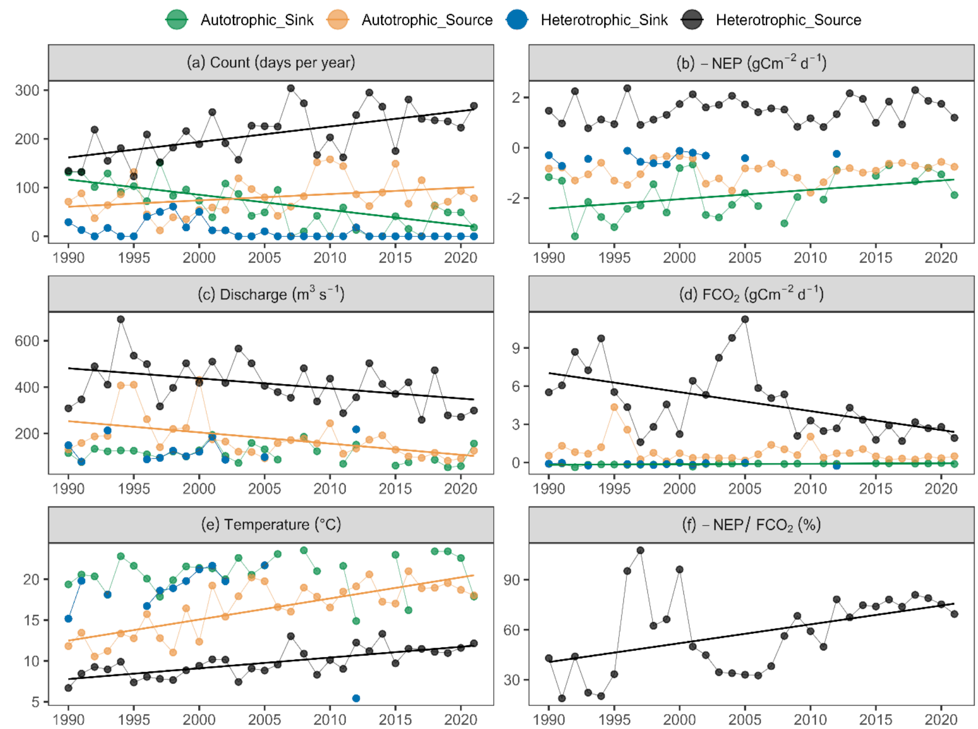

Figure 3. Long-term trends over 32 years of CO_2 fluxes, aquatic metabolism contribution, and hydroclimatic conditions on each trophlux state: a) occurrence per year, b) annual aquatic metabolism flux (–NEP), c) annual discharge, d) annual FCO_2, e) annual water temperature, f) –NEP/FCO_2. The points depicted on the graph were the annual averages. The regression lines were the Theil-Sen slopes with significant trends (p-value < 0.05).

3.4. Seasonal hysteresis of NEP and FCO_2 in relation to discharge

FCO_2 and NEP exhibited a similar clockwise hysteresis pattern in response to seasonal variations of discharge, i.e., higher fluxes in the rising discharge stage compared to the falling stage (Figure 4). Typically, hysteresis cycles started with FCO_2 minima and NEP maxima in July and August (mean discharge <150 m^3 s^{-1}, mean temperature 23 °C), with opposite peaks in January and February (mean discharge >500 m^3 s^{-1}, mean temperature 5 °C) (Figure 4a). As river discharge gradually increased from summer to winter, the river transitioned from an autotrophic to a heterotrophic state and from CO_2 sink to source. Subsequently, but along a different trajectory, the river shifted back to an autotrophic state during the spring-summer falling discharge stage (150–300 m^3 s^{-1}). During this time, however, the river continued to act as a CO_2 source, lasting two to three months (April–June) before returning to the FCO_2

https://doi.org/10.5194/egusphere-2025-1478
Preprint. Discussion started: 8 April 2025
© Author(s) 2025. CC BY 4.0 License.

minimum again in summer. The contribution of external sources largely mirrored these patterns (Figure 4.)

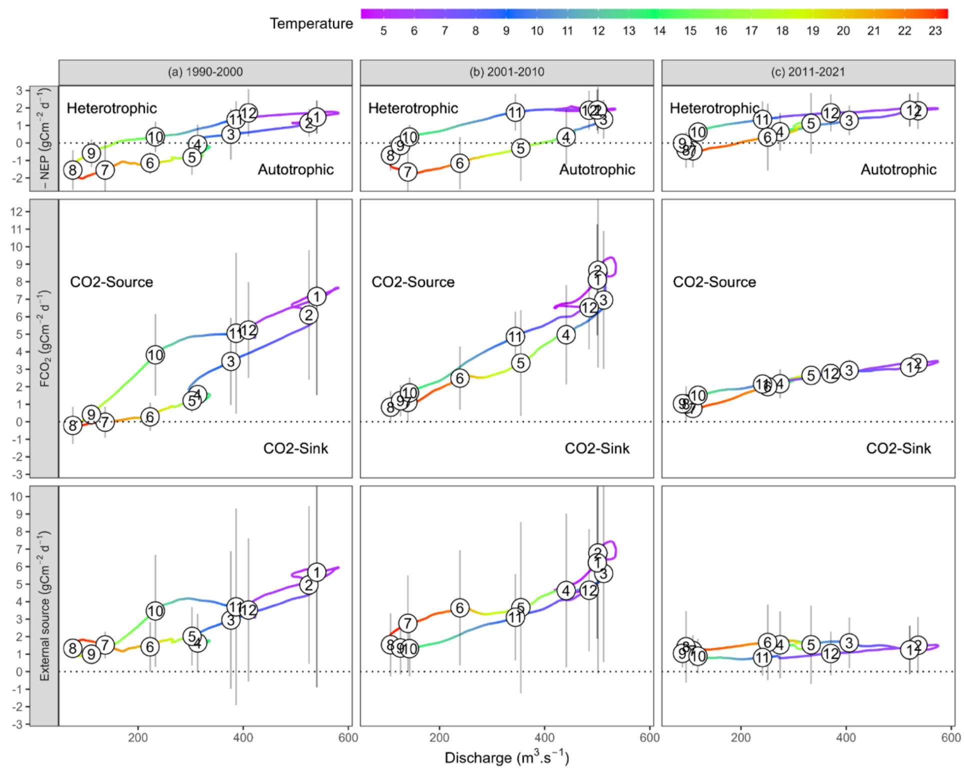

Figure 4. Hysteresis loops of –NEP, **FCO_2***, and external sources (FCO_2 + NEP) during the hydrological cycle in each decade 1990-2000, 2001-2010, and 2011-2021. The color lines are the daily average fluxes in each decade. The circle shape with numbers is the monthly average and standard deviation fluxes in each decade.*

The discharge trajectories of –NEP, FCO_2, and external sources varied across the three decades delineated by the change point analysis. In three decades, all hysteresis loops exhibited positive relationships with discharge, except the external CO_2 sources in 2011–2021. FCO_2 hysteresis magnitude at 300 $m^3 s^{-1}$ (autumn–spring) decreased from 3.2 g C $m^{-2} d^{-1}$ in 1990–2000 to -0.09 g C $m^{-2} d^{-1}$ in 2011–2021. The lack of FCO_2-discharge hysteresis 2011–2021 indicates a more predictable and linear relationship in recent years. Likewise, the magnitude of –NEP hysteresis at 300 $m^3 s^{-1}$ was weakest in recent years (0.68 g C $m^{-2} d^{-1}$), but unlike FCO_2, it exhibited a peak (2.12 g C $m^{-2} d^{-1}$) in 2001–2010 (Table 2).

https://doi.org/10.5194/egusphere-2025-1478
Preprint. Discussion started: 8 April 2025
© Author(s) 2025. CC BY 4.0 License.

The internal source contribution of FCO_2 (–NEP/FCO_2) at 300 $m^3 s^{-1}$ between spring and autumn had contrasting ratios, with a positive CO_2 contribution in autumn (14 – 34%) but a negative contribution in spring (-26%, i.e., CO_2 consumption) in 1990-2000 and 2001-2010 (Table 2). In 2011-2021, internal source contributions of FCO_2 in autumn and spring were both positive, 64% and 34%, respectively.

Table 2. The mean ± standard deviation fluxes of daily –NEP, FCO_2, external CO_2, and –NEP/FCO_2 in spring and autumn at the mean river discharge 300 ± 30 ($m^3 s^{-1}$).

	Flux*	1990–2000	2001–2010	2011–2021
River metabolism ($g\ C\ m^{-2} d^{-1}$)	$–NEP_{300}$ spring	-0.28 ± 0.41	-0.69 ± 0.11	0.83 ± 0.18
	$–NEP_{300}$ autumn	0.66 ± 0.15	1.43 ± 0.13	1.5 ± 0.06
	$–NEP_{300}$ hysteresis	0.94 ± 0.43	2.12 ± 0.17	0.68 ± 0.18
Total CO_2 fluxes ($g\ C\ m^{-2} d^{-1}$)	$FCO_{2\ 300}$ spring	1.55 ± 0.44	2.65 ± 0.15	2.42 ± 0.12
	$FCO_{2\ 300}$ autumn	4.77 ± 0.14	4.15 ± 0.25	2.34 ± 0.08
	$FCO_{2\ 300}$ hysteresis	3.22 ± 0.47	1.5 ± 0.29	-0.09 ± 0.14
External CO_2 flux ($g\ C\ m^{-2} d^{-1}$)	($FCO_{2\ 300}$+ NEP_{300}) spring	1.83 ± 0.2	3.34 ± 0.05	1.59 ± 0.14
	($FCO_{2\ 300}$+NEP_{300}) autumn	4.12 ± 0.05	2.72 ± 0.12	0.83 ± 0.05
	($FCO_{2\ 300}$+NEP_{300}) hysteresis	2.29 ± 0.2*	-0.62 ± 0.13**	-0.76 ± 0.15
–NEP/FCO_2 (%)	–NEP/$FCO_{2\ 300}$ spring	-26 ± 33%	-26 ± 5%	34 ± 6%
	–NEP/$FCO_{2\ 300}$ autumn	14 ± 3%	34 ± 1%	64 ± 1%
	–NEP/$FCO_{2\ 300}$ hysteresis	40 ± 34%	61 ± 5%	30 ± 6%

* The hysteresis flux is equal to the difference of flux in autumn and spring, i.e., 2.29 = 4.12–1.83, where the 300 subscript refers to the fact that these measurements are averages from mean discharge at 300 $m^3 s^{-1}$.
** Negative hysteresis flux indicates lower flux in autumn (rising waters stage), i.e., -0.62 = 2.72–3.34

4. Discussion

Our data analysis reveals important long-term changes in carbon fluxes of the Loire River. Re-oligotrophication led to an increase in the internal source contribution of FCO_2, supporting our hypothesis but for reasons that ran counter to our predictions. Indeed, under oligotrophic conditions and macrophyte dominance, –NEP/FCO_2 increased by fourfold overall under the heterotrophic-source state, with –NEP contributing up to 75% of FCO_2 at the monitoring station during the last decade (Figure 3). However, this change was largely due to decreases in total FCO_2 rather than an increase in the magnitude of –NEP. Instead, decreases in FCO_2 appeared to be due to an approximate halving of external CO_2 sources (Figure 5). Still, the timing of FCO_2 shifts, as detected by our change point analysis (ca. 2000 and 2010), broadly corresponded to our predictions based on previous studies (i.e., 2005 for trophic state

https://doi.org/10.5194/egusphere-2025-1478
Preprint. Discussion started: 8 April 2025
© Author(s) 2025. CC BY 4.0 License.

change and 2012 for metabolism change), suggesting similar drivers of external and internal CO_2. Finally, we observed clear support for our prediction of weaker discharge controls on FCO_2 and –NEP/FCO_2 based on hysteresis analysis. However, this appeared to be most strongly due to a weakened discharge-external CO_2 source link rather than a weakened discharge-internal CO_2 source link.

4.1. Trophlux states and their contribution to CO_2 emissions

Large river systems function predominately as a source of CO_2 to the atmosphere (Battin et al., 2023; Butman & Raymond, 2011; Cole et al., 2007; Raymond et al., 2013; Abril and Borges 2019), and CO_2 sink states are rarely observed, even in large eutrophic rivers (Raymond et al., 1997). However, our unique dataset revealed the commonality of CO_2 sink behavior in the Loire River and further highlighted the seasonal transitions among all four possible trophlux states and how these transitions varied annually and across decades (Figure 1, Figure 4). This finding challenges the conventional understanding of large rivers as persistent CO_2 sources and demonstrates how ecosystem metabolism can fundamentally alter carbon cycling patterns. The frequency of CO_2 sink conditions in the Loire River reveals an important but often overlooked aspect of river carbon budgets that may be significant for other large temperate systems undergoing similar environmental changes. We found that, regardless of the trophic or metabolic regime, the heterotrophic/source state was the most prevalent (47–66% of time), while the autotrophic-source state occurred for approximately a quarter of the year (17–26% of time). By contrast, the occurrence of the autotrophic-sink state depended strongly on the trophic and metabolic regime (7–29% of the time), with its decreasing decadal occurrence mirrored by the increasing decadal occurrence of the heterotrophic-source state (Figure 5). This shift in trophlux state dominance reflects the ecosystem's response to re-oligotrophication, where reduced nutrient availability has altered the balance between autotrophy and heterotrophy (Diamond et al., 2022). The declining prevalence of autotrophic-sink conditions indicates that the river's capacity to sequester atmospheric CO_2 has diminished with the transition from phytoplankton to macrophyte dominance. This demonstrates how long-term changes in trophic status can fundamentally alter carbon dynamics beyond simple changes in productivity rates.

https://doi.org/10.5194/egusphere-2025-1478
Preprint. Discussion started: 8 April 2025
© Author(s) 2025. CC BY 4.0 License.

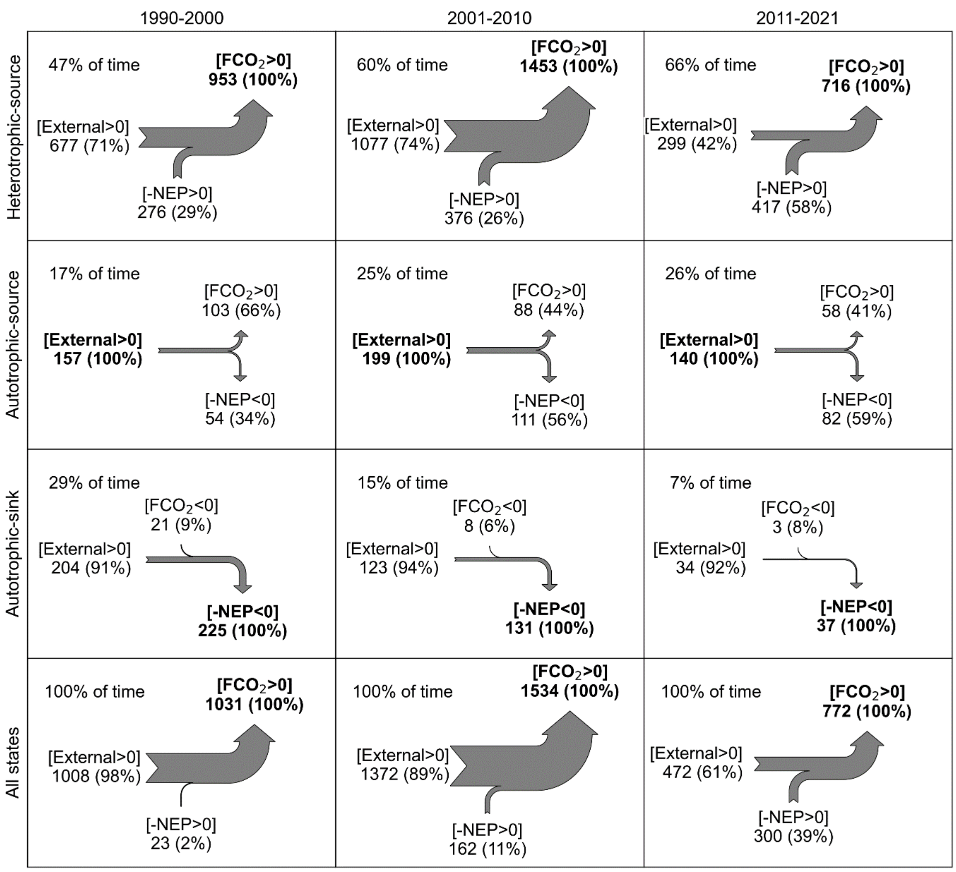

Figure 5. Annual CO_2 budget in three main trophlux states in 1990–2000, 2001–2010, and 2011–2021. All flux values are expressed in units of gC m^{-2} y^{-1}. The notation [FCO_2 > 0] denotes CO_2 emissions from rivers to the atmosphere, whereas [FCO_2 < 0] signifies CO_2 ingassing. The percentages in parentheses represent the proportion of each flux component, with the percentage calculated relative to the maximum flux component (shown in black bold).

4.2. Changes in CO_2 sources in relation to hydrology and re-oligotrophication

This work adds an important data point to our understanding of the contribution of internal and external sources to FCO_2 in large rivers. Despite this decades-old research question (Cole et al., 2001), the capacity to rigorously quantify the relative strength of these two fluxes is relatively recent (Bernal et al., 2022; Hotchkiss et al., 2015; Kirk & Cohen, 2023), and data in mid-sized and large rivers are still limited. Utilizing a dataset comprising 5 rivers with mean discharge >100 m^3 s^{-1}, Hotchkiss et al. (2015) estimated an NEP of -0.51 to -1.01 g C m^{-2} d^{-1} and –NEP/FCO_2 of 25% to 54%. Our results in the Loire

https://doi.org/10.5194/egusphere-2025-1478
Preprint. Discussion started: 8 April 2025
© Author(s) 2025. CC BY 4.0 License.

generally align with this range but further reveal that within a single river during a specific season (such as autumn or winter), the entire spectrum of these values can be observed.

While discharge is known to exert an influence on CO_2 dynamics, we showed that the temporal evolution of discharge is equally important to its magnitude. Depending on the season, our results caution that measurements at the same discharge may yield contrasting estimates of the internal source contribution (Table 2, Figure 4). This difference was mainly explained by the difference in NEP magnitude and not by differences in FCO_2. For example, at the same mean discharge, NEP in autumn during the rising stage was more negative, and the river was more heterotrophic than in spring during the falling stage. This difference was only partly explained by differences in daily temperature between the two seasons (R^2=0.29, Supplementary Figure S7). First autumn floods are known to mobilize labile organic matter in temperate rivers, whose drying river beds in summer accumulate plant litter from riparian vegetation (Coynel et al., 2005; Etcheber et al., 2007). In the Middle Loire, the emergence of large, fertile riverbanks during the summer dry season may lead to organic matter deposition that is easily remobilized in autumn. Indeed, Minaudo et al. (2015) observed that the heterotrophy in Middle Loire in autumn was strongly stimulated by a larger availability of biodegradable organic matter compared to spring. Such a seasonal hydrology-driven variability in river heterotrophy and associated CO_2 dynamics was also recently observed by Young et al. (2025) in the Upper Clark Fork River, USA. They reported pronounced seasonal variation in FCO_2 primarily linked to snowmelt-driven hydrological events mobilizing terrestrial carbon sources, reinforcing our observations that river CO_2 dynamics are strongly shaped by seasonal hydrological connectivity and terrestrial organic matter inputs.

Notably, Figure 4 reveals decadal changes in the magnitude of these hysteresis patterns. The FCO2 hysteresis magnitude at 300 $m^3 s^{-1}$ decreased dramatically from 3.2 g C $m^{-2} d^{-1}$ in 1990–2000 to -0.09 gC $m^{-2} d^{-1}$ in 2011–2021, indicating a weakening discharge-FCO_2 relationship in recent years. Similarly, external source hysteresis (bottom row, Figure 4) has flattened considerably in 2011-2021, suggesting diminished influence of terrestrial carbon inputs on seasonal CO_2 dynamics. As these insights would have been invisible without a high-frequency long-term dataset (Figure 1), we, therefore, encourage future efforts to capture seasonality and varying discharges in the measurement campaigns.

© Author(s) 2025. CC BY 4.0 License.

During the 1990–2000 decade, the Loire River had an annual CO_2 sink for almost half the years due to high rates of GPP. The occurrence of this state has gradually declined over the three decades (Table 1). In 1990–2000, the biogeochemical dynamics of the Loire River during the summer months coincided with long water residence times, shallow waters, low discharge, high water temperature, and high eutrophication (>200 µg chlorophyll-a L^{-1}) (Moatar et al., 1999, 2001). These conditions were similar to eutrophic lakes, which regularly act as CO_2 sinks (Bogard & Del Giorgio, 2016; He et al., 2022). In addition, large river autotrophs benefit from increased light penetration due to their greater width and from being less affected by external CO_2 sources (Hotchkiss et al., 2015). Our data show that in the Loire, the long-term shift from phytoplankton to macrophyte-dominance in 2005 has resulted in a decrease in NEP and greater heterotrophy. Diamond et al. (2021) showed that the changes in stream metabolism in Loire River in 2010–2012 were related to the shift of other state variables in 2005 (turbidity, nutrient concentrations, Corbicula fluminea densities, and chlorophyll-a), suggesting a decade lag for metabolism shift. Moreover, the increase in annual water temperature and decrease in annual river discharge have no direct relationship with these metabolic shifts (Figure S8), suggesting that their manifestation on the magnitude of NEP is insignificant.

4.3. Long-term changes in external CO_2 source

Contrary to our expectations, we observed a decreasing trend of FCO_2 attributable to an over 50% reduction in external CO_2 sources in the Loire River. At first glance, this may appear to be due to overall reductions in discharge and the magnitude of lateral CO_2 transport from groundwater and wetlands to the river (Abril & Borges, 2019). However, this linkage is more consistent with the seasonal variation (Figure S7) rather than the inter-annual variation (Figure S8). In addition, while the discharge can explain ca. 37-48% of the decay in FCO_2 (Figures S7 and S8), it only explains ca. 4-6% of the variation in external CO_2 source magnitude. Similarly, in a forested sandy watershed, Deirmendjian et al. (2018) reported that the export of CO_2 flux from groundwater to the stream was independent of stream discharge and relatively constant seasonally. This can be explained by the fact that higher discharge periods in these systems are associated with low dissolved CO_2 groundwater concentrations and vice-versa. Still,

https://doi.org/10.5194/egusphere-2025-1478
Preprint. Discussion started: 8 April 2025
© Author(s) 2025. CC BY 4.0 License.

to explain the >500 g C m^{-2} y^{-1} reduction in external CO_2 between 2001-2010 and 2011-2021, it seems clear that some reduction in groundwater CO_2 is occurring.

In regions with carbonate bedrock, weathering of carbonate minerals can significantly contribute to the CO_2 flux through the production of alkalinity (Vihermaa et al., 2014). Although this weathering reaction does not directly release CO_2, it provides bicarbonate ions (HCO_3^-), which can equilibrate with CO_2 and subsequently degas under certain conditions, influencing the CO_2 flux observed in groundwater and rivers. Additionally, the transfer of CO_2 to groundwater depends on the spatiotemporal connections between zones of maximal soil respiration and their intersection with the water table (Tsypin & Macpherson, 2012). If the water table remains disconnected from the topsoil where respiration is strongest, the transfer of soil CO_2 to groundwater becomes limited. Trend analysis of the groundwater table in France over the past 30 years shows low-frequency variations of multi-annual (~7 years) and decadal (~17 years) (Baulon et al., 2022). The groundwater table trend may explain the decay of annual external FCO_2 in the Loire River (Figure S9), although the spatiotemporal distribution of surface water and groundwater connections should be more deeply investigated to reach this conclusion. Still, we can observe that peaks in groundwater level tend to lead to peaks in external CO_2 by approximately 3 years (Figure S9). In addition, a study at a site located 20 km downstream from our study area in the Val d'Orléans fluviokarst aquifer reported that dissolved inorganic carbon flux from groundwater has decreased by about 20% along with the decrease of groundwater level between 2000 and 2020 (Binet et al., 2022). In addition, Binet et al., 2022 assessed that there was no significant change in the carbonate weathering rate at this aquifer, which is similar to the relatively stable alkalinity at the Loire River (Figure 2). These observations suggest a need for future efforts to focus on surface water-groundwater connections as they relate to river hydrology and carbon supply.

5. Conclusions

In the middle Loire River, three main trophlux states alternately occur in the hydrological year cycle, predominated by the heterotrophic-source state. The heterotrophic-source state contributes more than 90% of annual CO_2 emissions, with an average of 40% from internal contribution (–NEP). Besides, in the 1990s, the autotrophic-sink state was still common; however, this state has gradually disappeared in

© Author(s) 2025. CC BY 4.0 License.

recent years with the decline of phytoplankton, replaced by the dominance of macrophytes. Our analysis of seasonal hysteresis of NEP and CO_2 fluxes in relation to discharge indicates stronger heterotrophy in autumn during rising waters than in spring during the falling waters, and this is a part explained by river temperature but more likely due to the remobilization of organic matter in floodplains and secondary channels during the first floods.

We report a strong long-term decrease in CO_2 fluxes (-62% over the 32 years) but also an increase in the contribution of heterotrophy (–NEP) to this CO_2 outgassing flux. Although we can call for more DIC data acquisition in groundwaters, we must confess that the current dataset is far from sufficient to understand the transfer of carbon at the groundwater-river interface (Deirmendjian & Abril, 2018; Duvert et al., 2018) and therefore, future works are needed. We also suggest that new exploration of these types of datasets on large rivers and their extrapolation on river networks may help to understand better and predict the influence of global change on the balance between internal and external CO_2 production in the context of the global carbon budget.

Data availability

The hourly temperature, conductivity, dissolved oxygen, and pH data used in this study are owned by Électricité de France (EDF). Due to EDF's data-sharing policy, these data are not publicly available but can be accessed upon reasonable request by contacting EDF directly. Other publicly available datasets used include discharge (https://www.hydro.eaufrance.fr), water quality (www.naiades.eaufrance.fr).

Author Contribution

ANT led the manuscript effort. ANT, JSD, GA, and FM came up with the research question and designed the study approach. ANT and JSD conducted the data curation and preparation, and ANT conducted the statistical analyses. ANT wrote the paper with contributions from all authors.

Competing interests

The authors declare that they have no known competing financial interests or personal relationships that could have appeared to influence the work reported in this paper.

Acknowledgements

https://doi.org/10.5194/egusphere-2025-1478
Preprint. Discussion started: 8 April 2025
© Author(s) 2025. CC BY 4.0 License.

We express our gratitude to Electricité de France (EDF) for generously providing us with extensive long-term datasets in the Middle Loire River.

References

Abril, G., & Borges, A. V. (2019). Ideas and perspectives: Carbon leaks from flooded land: Do we need to replumb the inland water active pipe? Biogeosciences, 16(3), 769–784. https://doi.org/10.5194/bg-16-769-2019

Abril, G., Bouillon, S., Darchambeau, F., Teodoru, C. R., Marwick, T. R., Tamooh, F., Ochieng Omengo, F., Geeraert, N., Deirmendjian, L., Polsenaere, P., & Borges, A. V. (2015). Technical note: Large overestimation of pCO_2 calculated from pH and alkalinity in acidic, organic-rich freshwaters. Biogeosciences, 12(1), 67–78. https://doi.org/10.5194/bg-12-67-2015

Aho, K. S., Hosen, J. D., Logozzo, L. A., McGillis, W. R., & Raymond, P. A. (2021). Highest rates of gross primary productivity maintained despite CO_2 depletion in a temperate river network. Limnology and Oceanography Letters, 6(4), 200–206. https://doi.org/10.1002/lol2.10195

Amaral, J., Suhett, A., Melo, S., & Farjalla, V. (2013). Seasonal variation and interaction of photodegradation and microbial metabolism of DOC in black water Amazonian ecosystems. Aquatic Microbial Ecology, 70(2), 157–168. https://doi.org/10.3354/ame01651

Appling, A. P., Hall, R. O., Yackulic, C. B., & Arroita, M. (2018). Overcoming Equifinality: Leveraging Long Time Series for Stream Metabolism Estimation. Journal of Geophysical Research: Biogeosciences, 123(2), 624–645. https://doi.org/10.1002/2017JG004140

Battin, T. J., Lauerwald, R., Bernhardt, E. S., Bertuzzo, E., Gener, L. G., Hall, R. O., Hotchkiss, E. R., Maavara, T., Pavelsky, T. M., Ran, L., Raymond, P., Rosentreter, J. A., & Regnier, P. (2023). River ecosystem metabolism and carbon biogeochemistry in a changing world. Nature, 613(7944), 449–459. https://doi.org/10.1038/s41586-022-05500-8

Baulon, L., Allier, D., Massei, N., Bessiere, H., Fournier, M., & Bault, V. (2022). Influence of low-frequency variability on groundwater level trends. Journal of Hydrology, 606, 127436. https://doi.org/10.1016/j.jhydrol.2022.127436

Bernal, S., Cohen, M. J., Ledesma, J. L. J., Kirk, L., Martí, E., & Lupon, A. (2022). Stream metabolism sources a large fraction of carbon dioxide to the atmosphere in two hydrologically contrasting headwater streams. Limnology and Oceanography, 67(12), 2621–2634. https://doi.org/10.1002/lno.12226

Binet, S., Charlier, J.-B., Jozja, N., Défarge, C., & Moquet, J.-S. (2022). Evidence of long term biogeochemical interactions in carbonate weathering: The role of planktonic microorganisms and riverine bivalves in a large fluviokarst system. Science of the Total Environment, 842, 156823. https://doi.org/10.1016/j.scitotenv.2022.156823

Bogard, M. J., & Del Giorgio, P. A. (2016). The role of metabolism in modulating CO_2 fluxes in boreal lakes. Global Biogeochemical Cycles, 30(10), 1509–1525. https://doi.org/10.1002/2016GB005463

Butman, D., & Raymond, P. A. (2011). Significant efflux of carbon dioxide from streams and rivers in the united states. Nature Geoscience, 4(12), Article 12. https://doi.org/10.1038/ngeo1294

https://doi.org/10.5194/egusphere-2025-1478
Preprint. Discussion started: 8 April 2025
© Author(s) 2025. CC BY 4.0 License.

Cole, J. J., Cole, J. J., Caraco, N. F., & Caraco, N. F. (2001). Carbon in catchments: Connecting terrestrial carbon losses with aquatic metabolism. Marine and Freshwater Research, 52(1), 101. https://doi.org/10.1071/MF00084

Cole, J. J., Prairie, Y. T., Caraco, N. F., McDowell, W. H., Tranvik, L. J., Striegl, R. G., Duarte, C. M., Kortelainen, P., Downing, J. A., Middelburg, J. J., & Melack, J. (2007). Plumbing the global carbon cycle: Integrating inland waters into the terrestrial carbon budget. Ecosystems, 10(1), 171–184. https://doi.org/10.1007/s10021-006-9013-8

Coynel, A., Etcheber, H., Abril, G., Maneux, E., Dumas, J., & Hurtrez, J.-E. (2005). Contribution of small mountainous rivers to particulate organic carbon input in the bay of biscay. Biogeochemistry, 74(2), 151–171.

Deirmendjian, L., & Abril, G. (2018). Carbon dioxide degassing at the groundwater-stream-atmosphere interface: Isotopic equilibration and hydrological mass balance in a sandy watershed. Journal of Hydrology, 558, 129–143. https://doi.org/10.1016/j.jhydrol.2018.01.003

Diamond, J. S., Bernal, S., Boukra, A., Cohen, M. J., Lewis, D., Masson, M., Moatar, F., & Pinay, G. (2021). Stream network variation in dissolved oxygen: Metabolism proxies and biogeochemical controls. Ecological Indicators, 131(September), 108233. https://doi.org/10.1016/j.ecolind.2021.108233

Diamond, J. S., Moatar, F., Cohen, M. J., Poirel, A., Martinet, C., Maire, A., & Pinay, G. (2022). Metabolic regime shifts and ecosystem state changes are decoupled in a large river. Limnology and Oceanography, 67(S1). https://doi.org/10.1002/lno.11789

Dodds, W. K., & Smith, V. H. (2016). Nitrogen, phosphorus, and eutrophication in streams. Inland Waters, 6(2), 155–164. https://doi.org/10.5268/IW-6.2.909

Duvert, C., Butman, D. E., Marx, A., Ribolzi, O., & Hutley, L. B. (2018). CO2 evasion along streams driven by groundwater inputs and geomorphic controls. Nature Geoscience, 11(11), Article 11. https://doi.org/10.1038/s41561-018-0245-y

Etcheber, H., Taillez, A., Abril, G., Garnier, J., Servais, P., Moatar, F., & Commarieu, M.-V. (2007). Particulate organic carbon in the estuarine turbidity maxima of the gironde, loire and seine estuaries: Origin and lability. Hydrobiologia, 588(1), 245–259. https://doi.org/10.1007/s10750-007-0667-9

Floury, M., Delattre, C., Ormerod, S. J., & Souchon, Y. (2012). Global versus local change effects on a large european river. Science of the Total Environment, 441, 220–229. https://doi.org/10.1016/j.scitotenv.2012.09.051

He, H., Wang, Y., Liu, Z., Bao, Q., Wei, Y., Chen, C., & Sun, H. (2022). Lake metabolic processes and their effects on the carbonate weathering CO2 sink: Insights from diel variations in the hydrochemistry of a typical karst lake in SW china. Water Research, 222, 118907. https://doi.org/10.1016/j.watres.2022.118907

Hotchkiss, E. R., Hall Jr, R. O., Sponseller, R. A., Butman, D., Klaminder, J., Laudon, H., Rosvall, M., & Karlsson, J. (2015). Sources of and processes controlling CO2 emissions change with the size of streams and rivers. Nature Geoscience, 8(9), 696–699. https://doi.org/10.1038/ngeo2507

Humphreys, M. P., Lewis, E. R., Sharp, J. D., & Pierrot, D. (2022). PyCO2SYS v1.8: Marine carbonate system calculations in python. Geoscientific Model Development, 15(1), 15–43. https://doi.org/10.5194/gmd-15-15-2022

https://doi.org/10.5194/egusphere-2025-1478
Preprint. Discussion started: 8 April 2025
© Author(s) 2025. CC BY 4.0 License.

Hussain, Md., & Mahmud, I. (2019). pyMannKendall: A python package for non parametric mann kendall family of trend tests. Journal of Open Source Software, 4(39), 1556. https://doi.org/10.21105/joss.01556

Ibáñez, C., Caiola, N., Barquín, J., Belmar, O., Benito, X., Casals, F., Fennessy, S., Hughes, J., Palmer, M., Peñuelas, J., Romero, E., Sardans, J., & Williams, M. (2022). Ecosystem-level effects of re-oligotrophication and N:P imbalances in rivers and estuaries on a global scale. Global Change Biology, n/a(n/a). https://doi.org/10.1111/gcb.16520

Janssen, P., Chevalier, R., Chantereau, M., Dupré, R., Evette, A., Hémeray, D., Mårell, A., Martin, H., Rodrigues, S., Villar, M., & Greulich, S. (2023). Can vegetation clearing operations and reprofiling of bars be considered as an ecological restoration measure? Lessons from a 10-year vegetation monitoring program (loire river, france). Restoration Ecology, 31(3), e13704. https://doi.org/10.1111/rec.13704

Jones, J. B., Stanley, E. H., & Mulholland, P. J. (2003). Long-term decline in carbon dioxide supersaturation in rivers across the contiguous united states. Geophysical Research Letters, 30(10), 2003GL017056. https://doi.org/10.1029/2003GL017056

Kirk, L., & Cohen, M. J. (2023). River corridor sources dominate CO2 emissions from a lowland river network. Journal of Geophysical Research: Biogeosciences, 128(1), e2022JG006954. https://doi.org/10.1029/2022JG006954

Koehler, B., Landelius, T., Weyhenmeyer, G. A., Machida, N., & Tranvik, L. J. (2014). Sunlight-induced carbon dioxide emissions from inland waters. Global Biogeochemical Cycles, 28(7), 696–711. https://doi.org/10.1002/2014GB004850

Lynch, J. K., Beatty, C. M., Seidel, M. P., Jungst, L. J., & DeGrandpre, M. D. (2010). Controls of riverine CO 2 over an annual cycle determined using direct, high temporal resolution p CO 2 measurements. Journal of Geophysical Research: Biogeosciences, 115(G3), 2009JG001132. https://doi.org/10.1029/2009JG001132

Millero, F. J. (1979). The thermodynamics of the carbonate system in seawater. Geochimica et Cosmochimica Acta, 43(10), 1651–1661. https://doi.org/10.1016/0016-7037(79)90184-4

Minaudo, C., Meybeck, M., Moatar, F., Gassama, N., & Curie, F. (2015). Eutrophication mitigation in rivers: 30 years of trends in spatial and seasonal patterns of biogeochemistry of the loire river (1980–2012). Biogeosciences, 12(8), 2549–2563. https://doi.org/10.5194/bg-12-2549-2015

Moatar, F., Descy, J.-P., Rodrigues, S., Souchon, Y., Floury, M., Grosbois, C., Minaudo, C., Leitao, M., Wantzen, K. M., & Bertrand, F. (2022). Chapter 7—The loire river basin. In K. Tockner, C. Zarfl, & C. T. Robinson (Eds.), Rivers of Europe (Second Edition) (pp. 245–271). Elsevier. https://doi.org/10.1016/B978-0-08-102612-0.00007-9

Moatar, F., Fessant, F., & Poirel, A. (1999). pH modelling by neural networks. Application of control and validation data series in the middle loire river. Ecological Modelling, 120(2–3), 141–156. https://doi.org/10.1016/S0304-3800(99)00098-8

Moatar, F., & Meybeck, M. (2005). Compared performances of different algorithms for estimating annual nutrient loads discharged by the eutrophic River Loire. Hydrological Processes, 19(2), 429–444. https://doi.org/10.1002/hyp.5541

Moatar, F., Miquel, J., & Poirel, A. (2001). A quality-control method for physical and chemical monitoring data. Application to dissolved oxygen levels in the river loire (france). Journal of Hydrology, 252(1–4), 25–36. https://doi.org/10.1016/S0022-1694(01)00439-5

https://doi.org/10.5194/egusphere-2025-1478
Preprint. Discussion started: 8 April 2025
© Author(s) 2025. CC BY 4.0 License.

NOAA. (n.d.). Trends in atmospheric carbon dioxide. Global Monitoring Laboratory - Carbon Cycle Greenhouse Gases. https://gml.noaa.gov/ccgg/trends/data.html

Raymond, P. A., Caraco, N. F., & Cole, J. J. (1997). Carbon dioxide concentration and atmospheric flux in the hudson river. Estuaries, 20(2), 381. https://doi.org/10.2307/1352351

Raymond, P. A., Hartmann, J., Lauerwald, R., Sobek, S., McDonald, C., Hoover, M., Butman, D., Striegl, R., Mayorga, E., Humborg, C., Kortelainen, P., Dürr, H., Meybeck, M., Ciais, P., & Guth, P. (2013). Global carbon dioxide emissions from inland waters. Nature, 503(7476), 355–359. https://doi.org/10.1038/nature12760

Raymond, P. A., Zappa, C. J., Butman, D., Bott, T. L., Potter, J., Mulholland, P., Laursen, A. E., McDowell, W. H., & Newbold, D. (2012). Scaling the gas transfer velocity and hydraulic geometry in streams and small rivers. Limnology and Oceanography: Fluids and Environments, 2(1), 41–53. https://doi.org/10.1215/21573689-1597669

Reed, A. P., Stets, E. G., Murphy, S. F., & Mullins, E. A. (2021). Aquatic-terrestrial linkages control metabolism and carbon dynamics in a mid-sized, urban stream influenced by snowmelt. Journal of Geophysical Research: Biogeosciences, 126(9), e2021JG006296. https://doi.org/10.1029/2021JG006296

Rocher-Ros, G., Harms, T. K., Sponseller, R. A., Väisänen, M., Mörth, C.-M., & Giesler, R. (2021). Metabolism overrides photo-oxidation in CO2 dynamics of Arctic permafrost streams. Limnology and Oceanography, 66(S1), S169–S181. https://doi.org/10.1002/lno.11564

Rocher-Ros, G., Sponseller, R. A., Bergström, A., Myrstener, M., & Giesler, R. (2020). Stream metabolism controls diel patterns and evasion of CO2 in arctic streams. Global Change Biology, 26(3), 1400–1413. https://doi.org/10.1111/gcb.14895

Seabold, S., & Perktold, J. (2010). Statsmodels: Econometric and statistical modeling with python. 92–96. https://doi.org/10.25080/Majora-92bf1922-011

Truong, C., Oudre, L., & Vayatis, N. (2020). Selective review of offline change point detection methods. Signal Processing, 167, 107299. https://doi.org/10.1016/j.sigpro.2019.107299

Tsypin, M., & Macpherson, G. L. (2012). The effect of precipitation events on inorganic carbon in soil and shallow groundwater, konza prairie LTER site, NE kansas, USA. Applied Geochemistry, 27(12), 2356–2369. https://doi.org/10.1016/j.apgeochem.2012.07.008

Van Vliet, M. T. H., Franssen, W. H. P., Yearsley, J. R., Ludwig, F., Haddeland, I., Lettenmaier, D. P., & Kabat, P. (2013). Global river discharge and water temperature under climate change. Global Environmental Change, 23(2), 450–464. https://doi.org/10.1016/j.gloenvcha.2012.11.002

Vihermaa, L. E., Waldron, S., Garnett, M. H., & Newton, J. (2014). Old carbon contributes to aquatic emissions of carbon dioxide in the Amazon. Biogeosciences, 11(13), 3635–3645. https://doi.org/10.5194/bg-11-3635-2014

Wallin, M. B., Audet, J., Peacock, M., Sahlée, E., & Winterdahl, M. (2020). Carbon dioxide dynamics in an agricultural headwater stream driven by hydrology and primary production. Biogeosciences, 17(9), 2487–2498. https://doi.org/10.5194/bg-17-2487-2020

Young, F. L., Colman, B. P., Carter, A. M., Fiejó De Lima, R., Shangguan, Q., Payn, R. A., & DeGrandpre, M. D. (2025). Variability and Controls of p CO2 and Air-Water CO2 Fluxes in a Temperate River. Journal of Geophysical Research: Biogeosciences, 130(2), e2024JG008434. https://doi.org/10.1029/2024JG008434

https://doi.org/10.5194/egusphere-2025-1478
Preprint. Discussion started: 8 April 2025
© Author(s) 2025. CC BY 4.0 License.

Zhang, T., Li, J., Pu, J., Martin, J. B., Khadka, M. B., Wu, F., Li, L., Jiang, F., Huang, S., & Yuan, D. (2017). River sequesters atmospheric carbon and limits the CO2 degassing in karst area, southwest China. Science of the Total Environment, 609, 92–101. https://doi.org/10.1016/j.scitotenv.2017.07.143